

This discussion paper is/has been under review for the journal Hydrology and Earth System Sciences (HESS). Please refer to the corresponding final paper in HESS if available.

# Quantification of the Beauce's Groundwater contribution to the Loire River discharge using satellite infrared imagery

E. Lalot<sup>1</sup>, F. Curie<sup>1</sup>, V. Wawrzyniak<sup>2</sup>, S. Schomburgk<sup>3</sup>, H. Piegay<sup>2</sup>, and F. Moatar<sup>1</sup>

<sup>1</sup>Laboratoire GEHCO, UFR sciences et techniques, Université François Rabelais, Tours, France

<sup>2</sup>Plateforme ISIG, Ecole Normale Supérieure de Lyon, Université de Lyon, Lyon, France

<sup>3</sup>Dir. Eau Environnement et Ecotechnologies, Bureau de Recherches Géologiques et Minières (BRGM), Orléans, France

Received: 19 December 2014 – Accepted: 31 January 2015 – Published: 16 February 2015

Correspondence to: E. Lalot (eric.lalot@gmail.com)

Published by Copernicus Publications on behalf of the European Geosciences Union.

2047

## Abstract

Seven Landsat Thermal InfraRed (TIR) images, taken over the period 2000–2010, were used to establish longitudinal temperature profiles of the middle Loire River, where it flows above the Beauce aquifer. Results showed that 75 % of the temperature differences, between in situ observations and TIR image based estimations, remained within the  $\pm 1^\circ\text{C}$  interval. The groundwater discharge along the River course was quantified for each identified groundwater catchment areas using a heat budget based on the Loire River temperature variations, estimated from the TIR images. The main discharge area of the Beauce aquifer into the Loire River was located between river kilometers 630 and 650. This result confirms what was obtained using a groundwater budget and spatially locates groundwater input within the Middle sector of the Loire River. According to the heat budgets, groundwater discharge is higher during winter period ( $13.5\text{ m}^3\text{ s}^{-1}$ ) than during summer ( $5.3\text{ m}^3\text{ s}^{-1}$ ). Groundwater input is also higher during the flow recession periods of the Loire River.

## 1 Introduction

Water temperature is a key factor for aquatic fauna (Ward, 1992; Caissie, 2006). For instance, it controls oxygen's dissolution, a key parameter for aquatic organisms. River temperature is controlled by many factors such as solar radiation, air temperature or groundwater discharge (Webb and Zhang, 1997, 1999; Hannah et al., 2004). However, quantifying the respective influence of these factors is often difficult, since temperature profiles of the river course have first to be established.

Since the late 1990's Thermal InfraRed images (TIR) have been used to determine river water temperature along sections ranging from tens to hundreds of kilometers (Torgersen et al., 2001; Handcock et al., 2006, 2012). Until now, TIR images of water courses have mainly been used to: (i) identify cold refuges for fish in summertime (Belknap and Naiman, 1998; Torgersen et al., 1999; Tonolla et al., 2010; Monk et al.,

2048

2013), (ii) study the thermal variability of rivers or alluvial floodplains and locate areas of similar thermal characteristics (Smikrud et al., 2008; Tonolla et al., 2010; Wawrzyniak et al., 2012, 2013), (iii) validate river temperature models (Boyd and Kasper, 2003; Cristea and Burges, 2009).

5 However, most of these studies are based on airborne TIR images. Studies based on satellite TIR images are scarce, mostly because the spatial resolution of these images is usually poor. In the case of the Landsat 7 satellite, one pixel of the TIR image represents  $60\text{ m} \times 60\text{ m}$  on the ground surface. Therefore, only a few large river courses could be studied using TIR satellite images, as it was considered that the river width  
10 had to exceed 3 images pixels to allow enough accuracy in water temperature estimation (Handcock et al., 2006; Wawrzyniak et al., 2012). However, Landsat satellite images have the advantage over airborne images of being freely available at different dates. As the ground covered by one single satellite image would take time to be covered using air transportation, longitudinal thermal profiles derived from TIR satellite  
15 images also show less bias due to change in water temperature during sampling time.

Although it has been shown that groundwater discharge may have a significant influence on surface water temperature (Hannah et al., 2004; Webb and Zhang, 1997, 1999), this influence has seldom been studied based on TIR images (Loheide and Gorelick, 2006; Burckholder et al., 2007; Wang et al., 2008; Danielescu et al., 2009;  
20 Mallast et al., 2014). Only one paper describes a test to quantify the groundwater discharge in a small stream, based on the longitudinal temperature profile established from the airborne TIR images (Loheide and Gorelick, 2006). To the authors' knowledge, groundwater discharge to rivers has not been observed or quantified before, using satellite TIR images.

25 Along the middle Loire River, where several nuclear power plants are located, the understanding of the water temperature evolution is an operational issue for "Electricité De France" (EDF). It has been shown that between the nuclear power plant of Dampierre and Saint-Laurent des Eaux the Loire temperature is influenced by the groundwater discharge from the Beauce aquifer and the Val d'Orléans hydrogeologi-

2049

cal system (Alberic and Lepiller, 1998; Alberic, 2004; Moatar and Gailhard, 2006). The average discharge of the Beauce aquifer has already been quantified using hydrogeological numerical modelling (Monteil, 2011; Flipo et al., 2012) and it was found to be circa  $10\text{ m}^3\text{ s}^{-1}$  on inter annual average. However, until now, the groundwater discharge  
5 has not been well located or quantified based on field measurement data.

The main goals of this study were to test the abilities of Landsat satellite thermal infrared images (i) to accurately determine water temperature in river having a width under 180 m, (ii) to characterize the evolution of temperature along a 135 km section of the middle Loire River overlying the Beauce aquifer between Dampierre and Blois, (iii) to  
10 locate and quantify the groundwater discharge's contribution of the Beauce aquifer into the Loire River.

## 2 Study area

The study site is the Loire River between Gien and Blois (a 135 km reach) which overlies the Beauce aquifer (Fig. 1). The catchment area of the Loire River at Gien  
15 is  $35\,000\text{ km}^2$  and the river slope is  $0.4\text{ m km}^{-1}$  in the studied section (Latapie et al., 2014).

The river flow is measured daily in Gien, Orléans and Blois, respectively at river kilometers 560, 635 and 695 (Banque HYDRO: [www.hydro.eaufrance.fr](http://www.hydro.eaufrance.fr)). Over the 1964–2011 period, the average flow in Orléans is  $345\text{ m}^3\text{ s}^{-1}$ , the average flow in August is  
20  $95\text{ m}^3\text{ s}^{-1}$  and the average flow in January is  $553\text{ m}^3\text{ s}^{-1}$ .

The width of the wet section of the middle Loire River ranges between 200 and 450 m (Latapie et al., 2014) which is higher than the three image pixels (180 m) threshold. However, during low flow periods, the Loire River locally forms several branches and the river main branch width can be as low as 50 m. During low flow periods, the average  
25 river depth is about 1 m in this section. The main weirs (natural and artificial) along the Loire River are located at river kilometers 571, 603, 635, 661, and 670, where the river water level shows a drop of just over 1 m at low flow.

2050

On the study area the climate is temperate. The mean annual air temperature in Orléans is 11 °C. The cold season lasts from mid-November to early March, with an average air temperature of 4.0 °C (data from Météo France at Orléans station for the period 1961–1990). The warm season lasts from late May to early September, with an average air temperature of 17.2 °C.

The water temperature of the Loire River is influenced by several factors: (i) atmospheric heat fluxes from direct solar radiations, diffuse solar radiation, latent heat exchange, conduction and water emitted radiations, (ii) groundwater discharge from the Beauce aquifer and Val d'Orléans hydrosystem (Alberic, 2004; Gutierrez and Binet, 2010), (iii) warm water originating from the cooling system of the nuclear power plants of Dampierre and Saint-Laurent des Eaux (average discharge of  $2 \text{ m}^3 \text{ s}^{-1}$  by nuclear reactors). However, the influence of the nuclear power plant on the Loire River temperature is low, the heat being removed through cooling towers. The median temperature rise of the Loire River between the upstream and downstream parts of the nuclear power plants is 0.1 °C with a 90th percentile of 0.3 °C (Bustillo et al., 2014). The greatest increase due to nuclear power plants in the Loire River temperature is observed in winter at low flow ( $< 1 \text{ °C}$ ), (iv) flows from the tributaries. The catchment area of the Loire River between Gien and Blois is around  $5600 \text{ km}^2$ , (a 16 % increase of the Loire River catchment area over the 135 km reach). The influence of the tributaries on the Loire River temperature is considered negligible in this section of the Loire River, since the water temperature of the tributaries is usually close to the Loire River temperature (Moatar and Gailhard, 2006). However, the main tributary of the Loire River, the Loiret River, drains water originating from both the Beauce aquifer and the Loire River (Alberic, 2004; Binet et al., 2011) and is very short (6 km). The influence from the Loiret is therefore difficult to separate from that of the Beauce aquifer.

2051

### 3 Material and methods

#### 3.1 Data

Seven satellite images from the Landsat 7 ETM+, presenting cloud cover under 10 %, were extracted from the period 1999–2010 (<http://earthexplorer.usgs.gov/>) (Table 1). 5 images were available in the warm season and 2 in the cold season. They were taken at 12:30 LT in summertime and 11:30 LT in wintertime. Each image covered the entire Loire River course between Gien and Blois.

Water temperatures of the Loire River are monitored by EDF upstream of the nuclear power plant of Dampierre (river kilometer 571) and Saint-Laurent des Eaux (river kilometer 670) on an hourly basis. In the cold season, the average observed daily water temperature, on the days when the images were taken, was 5.2 °C. In the warm season, it was 23.7 °C.

River flows measured in Orléans, on the days the images were taken, were comprised between  $61$  and  $478 \text{ m}^3 \text{ s}^{-1}$ . On 6 out of the 7 dates for which the images were taken, the Loire River flow was lower than the average flow.

#### 3.2 From the satellite TIR images to the Loire River temperature longitudinal profiles

TIR image pixels corresponding solely to water were first identified using a threshold based on the TM 8 band of the Landsat images ( $0.52$  to  $0.9 \mu\text{m}$ ; USGS, 2013). Only pixel values below the threshold were kept. The aerial images in the visible range from BD Ortho, from the “Institut National de l'information Géographique et forestière” (IGN), were used to set the threshold value for each image by comparing the TM 8 band to the Loire water course in places where it was known and not altered with time. The Carthage database from the IGN, which maps all the French watercourses in the form of lines, enabled the further separation of the water pixels belonging to the Loire River

2052



where RA is the atmospheric radiations, RS the solar radiations, RE the emitted radiations, CV the conduction, and CE the condensation/evaporation.

The atmospheric parameters extracted from the SAFRAN database from Météo France (Quintana-Segui et al., 2008) were averaged along the successive Loire River sections considered. Every atmospheric factor was averaged over the 24 h period preceding the taking of the infrared image. This choice is questionable as the water temperature in the Loire River may be influenced by changes in atmospheric factors over a longer time period. However, water travel time between Gien and Blois is about 1 to 1.5 days on the dates when the images were taken. Atmospheric parameters should therefore not be integrated over a period exceeding a day.

As the Loire River course is large, no shading from the alluvial forest was taken into account.

### 3.4 Groundwater discharge estimation – groundwater budget

Average groundwater discharge into the Loire River was calculated using groundwater budget per groundwater catchment areas over the 1998–2007 period. Effective rainfall was then calculated for each catchment area using Turc formulae. The useable ground reserves are available at the municipality-scale and 1000 weather stations were considered in order to spatialize the atmospheric parameters. Effective rainfall was further separated between infiltration to the groundwater and surface runoff using the IDPR index (Mardhel et al., 2004; Putot and Bichot, 2007). Known groundwater withdrawals, obtained from the Water Agencies, were then removed from the calculated infiltrated water. In steady state condition, the average infiltration rate in the aquifers corresponds to the groundwater discharge into the Loire River.

2055

## 4 Results

### 4.1 Temperature accuracy

The comparison between the in situ and TIR derived temperatures shows that, on average, the TIR images tend to overestimate the Loire River water temperature in winter (+0.3 °C) and to underestimate it in summer (–1 °C).

Over 75 % of the TIR derived temperatures are comprised between  $\pm 1$  °C of the temperature measured directly into the river (11 times out of 14: Fig. 2). But the temperature difference exceeds 1.5 °C on 29 May 2003 and on 29 July 2002 at the Dampierre station and on 29 July 2002 at Saint-Laurent des Eaux.

To assess the influence of the nature of the water pixels (pure or non-pure), tests were carried out. In the case where, for a 200 m section of the Loire River, pure water pixels exist, temperature was estimated for both pure water pixels and non-pure water pixels. The linear regression between temperature estimated with pure water pixels and temperature estimated with non-pure water pixels was drawn and the standard deviation of the residuals of the regression line was calculated. The standard deviation is found to be comprised between 0.18 and 0.21 °C and the slope of the regression line is comprised between 0.98 and 1.01. Therefore, taking into account non-pure water pixels does not seem to induce an important bias in the case of the Loire River.

However, when the number of water pixels in a 200 m section of the Loire River decreases (small river width), the standard deviation of the observed temperature increases notably (Table 3). Peak temperature values along the longitudinal thermal profile may therefore appear in places where the main river branch is particularly narrow. This phenomenon is mostly due to the uncertainties inherent to the satellite sensor. Uncertainty is reduced by averaging. The more pixels are considered over a section, the lower the uncertainty is.

2056





ature estimation. As a result, important uncertainties are attached to the estimated groundwater discharge when the length of the river section considered is small. Then, there are uncertainties inherent to the heat budget method used. Factors such as bed friction, heat conduction through the bed, or hyporheic exchange are not considered. However, for that kind of slow flowing river, the influence of bed friction is assumed to be low, especially in summer (Evans et al., 1998). Similarly, heat conduction through the bed usually plays a minor role in the global river heat budget (Hannah et al., 2008). The effect of heat conduction and hyporheic flows can be confused with the groundwater discharge which probably leads to a small overestimation of the groundwater discharge. The water travel time along the river is not taken into account in the heat budget either. As a result, the influence of the local atmospheric conditions over the river temperature tends to be slightly overestimated. Uncertainties are also attached to the groundwater discharge calculated with the groundwater budget. Then, the groundwater discharge estimate given by the groundwater budget method is an average value over a 10 year period. In contrast, only 7 TIR images are taken into account in this study and the average discharge estimated using these images is therefore related to the sampling date. It may suffice to explain the difference between the average estimated groundwater flow using the heat budget and the flow calculated by the groundwater budget method. Despite all the uncertainties, the groundwater discharge estimated using the heat budget stays in the order of magnitude of the discharge calculated with the groundwater budget. At maximum, the groundwater discharge rate, estimated with the heat budget, overestimate, or underestimate, by less than  $1 \text{ m}^3 \text{ s}^{-1} \text{ km}^{-1}$  the discharge calculated by the groundwater budget. The average groundwater discharge calculated by the groundwater budget for the inter-annual period is always within the range of variation of the groundwater discharge estimated using the river heat budget. The shape of the estimated average groundwater discharge curve along the Loire River is also relatively close to the one calculated by the groundwater budget method (coefficient of determination  $r^2 = 0.82$ ).

2061

On the upstream part of the Loire River, i.e. from river kilometer 560 to 635, the groundwater discharge estimated from the heat budget appears to be small (less than  $0.3 \text{ m}^3 \text{ s}^{-1} \text{ km}^{-1}$ ), except for some dates around river kilometer 564. It is known that between river kilometers 610 and 625 the Loire River loses water through the Val d'Orléans karstic system (Alberic, 2004; Binet et al., 2011). It should be noted that the high standard deviation of the estimated discharge near river kilometer 564 may be explained not only by real variations of the discharge rate, as highlighted by the groundwater budget, but also by bias resulting from the small length of the corresponding section. A first thermal anomaly appears downstream of river kilometer 620. From river kilometer 635 to river kilometer 645 the groundwater discharge estimated with the heat budget is comprised between  $0.3$  and  $1.5 \text{ m}^3 \text{ s}^{-1} \text{ km}^{-1}$ . This section corresponds to a known discharge area of the Beauce aquifer and the Val d'Orléans hydrosystem (Desprez and Martin, 1976; Gonzalez, 1991; Binet et al., 2011) that is also identified by the groundwater budget. It is interesting to note that along the Loire River, the maximum exchange rates estimated occur at times where the river flow decreases between two consecutive days, while the lowest exchange rate is estimated when the river flow increases (Fig. 6). Maximum groundwater discharge is also estimated in winter ( $13.5$  compared to  $5.3 \text{ m}^3 \text{ s}^{-1}$  in summer), when groundwater level is at its highest. It is known that temporal changes in river water level can lead to important modifications in exchange rates and exchange directions (Sophocleous, 2002). During a rise in river water level, water from the river can flow into the lateral aquifer while the opposite phenomenon happens at low river flow. Thus, the variation in estimated exchange rates is likely to have a physical basis. An exchange rate of  $11.5$  to  $12.5 \text{ m}^3 \text{ s}^{-1}$  was calculated at la Chapelle Saint-Mesmin (river kilometer 642), using geo-chemical tracers during the summer 1986 (Gonzalez, 1991). It is higher than the maximum groundwater discharge estimated in summer using the heat budget ( $7.5 \text{ m}^3 \text{ s}^{-1}$ ). Therefore, the high discharge rates estimated using the heat budget are plausible. The satellite TIR images allow to locate the main groundwater discharge area precisely, along the right bank of the Loire River and 2 to 3 km upstream from the confluence with the Loiret

2062



(Fig. 7). On the downstream part of the Loire River, between river kilometers 650 and 680, groundwater discharge decreases according to both estimations (heat budget and groundwater budget). Then, downstream of river kilometer 680, groundwater discharge estimated with the groundwater budget increases again. However, even though an increase in the median discharge estimated with the heat budget is observed, its value stays negative (Fig. 5). This difference may be explained by the limitations of the heat budget employed, since a drop in water temperature is observed on all summer thermal profiles. However, this drop does not start at the same location depending on dates. The main groundwater outlet location seems to change with time and to be located on the downstream part of the section considered (near Blois).

The change in the groundwater discharge rate with time could explain why the river temperature may either rise or drop between river kilometers 645 and 665, or between river kilometers 570 and 620. However, atmospheric factors are also likely to play a role, even though atmospheric data available do not offer a satisfactory explanation for this phenomenon. The influence of warm water discharges from the nuclear power plant on the longitudinal temperature profile is not noticeable either, as no sudden temperature rise is observed at the nuclear plant locations. In the case of Saint-Laurent des Eaux, warm water discharges may nevertheless contribute for some part to the global temperature rise observed between river kilometers 670 and 680 (Figs. 3 and 4), but the temperature rise begins upstream of the power plant. Similarly, no sudden temperature variations could be explained by weirs across the river course and changes in the river slope, although abrupt temperature changes near weirs have been observed on the Ain River in France (Wawrzyniak, 2012), based on airborne TIR images. This could be explained by the small reservoir capacity of the Loire River upstream of the weirs (Casado et al., 2013), and probably by the low spatial resolution of the satellite TIR images.

2063

## 6 Conclusion

Temperatures of the middle Loire River were estimated using Thermal InfraRed (TIR) Landsat images. With no atmospheric correction considered and taking into account non-pure water pixels, temperature differences, between in situ observation and TIR images based estimation, remains within the interval defined in previous studies (i.e. 75 % of these differences being in the  $\pm 1^\circ\text{C}$  interval). Therefore, this study shows that river temperature may be studied from satellite TIR images even when river width falls below the three pixels' width threshold (i.e.  $< 180\text{ m}$ ). However, the river temperature can be seriously underestimated at low flow and when water temperature is high (difference of over  $2^\circ\text{C}$ ).

We demonstrate that groundwater discharge to a large river can be estimated using satellite images. The groundwater discharge was estimated along the Loire River using both a heat budget based on the longitudinal temperature profiles established from the TIR images, and a groundwater budget on the successive groundwater catchment areas. The evolution of the groundwater discharge rate along the Loire River is found to be similar according to both methods. The main discharge area of the Beauce aquifer into the Loire River is located between river kilometers 635–645 (close to la Chapelle Saint-Mesmin).

According to the TIR images, the groundwater discharge appears to be higher in wintertime ( $13.5\text{ m}^3\text{ s}^{-1}$ ) than in summertime ( $5.3\text{ m}^3\text{ s}^{-1}$ ). It is also found to be higher when the Loire River flow decreases between 2 consecutive days. Our TIR images underline that instantaneous groundwater discharges are highly variable with time. Therefore, average discharge is not sufficient to predict the observed changes in water temperature along the river course.

To assess the consistency and robustness of the results, further studies could be conducted using more sophisticated modelling of both the groundwater discharge and the stream temperature.

2064

*Acknowledgements.* This work was part of the scientific program “Control factors of river temperature at regional scale in the Loire catchment” funded by European funds (FEDER, Fonds Européens de Développement Régional), Etablissement Public Loire and the Loire River Basin authority (Agence de l’Eau Loire Bretagne). The calculation of groundwater fluxes using groundwater budget was also funded by Electricité De France (EDF) and monitored by Mohamed Krimissa from EDF.

We thank Alain Poirel from EDF for the hourly Loire River temperature measurements on the days of the images. We also thank Météo France for the SAFRAN database. We are grateful to Nicolas Flipo and Fulvia Baratelli from Mines Paris Tech for their helpful comments on our results. We finally thank the team of assessment and evaluation of knowledge on water of the BRGM water department and especially Alexandre Brugeron for their help in characterizing groundwater catchment areas and groundwater fluxes.

## References

- Alberic, P.: River backflooding into a karst resurgence (Loiret, France), *J. Hydrol.*, 286, 194–202, 2004.
- Alberic, P. and Lepiller, M.: Oxydation de la matière organique dans un système hydrologique karstique alimenté par des pertes fluviales (Loiret, France), *Water Resour.*, 32, 2051–2064, 1998.
- Barsi, J. A., Barker, J. L., and Schott, J. R.: An atmospheric correction parameter calculator for a single thermal band earth-sensing instrument, in: *Geoscience and Remote Sensing Symposium, IGARSS’03, Proceedings, IEEE International*, 21–25 July, Toulouse, France, 3014–3016, 2003.
- Belknap, W. and Naiman, R. J.: A GIS and TIR procedure to detect and map wall-base channels in Western Washington, *J. Environ. Manage.*, 52, 147–160, 1998.
- Binet, S., Auterives, C., and Charlier, J. B.: Construction d’un modèle hydrogéologique d’étiage sur le val d’Orléans, rapport final, ICERE, Orléans, France, 2011.
- Boyd, M. and Kasper, B.: *Analytical Methods for Dynamic Open Channel Heat and Mass Transfer: Methodology for Heat Source Model Version 7.0*, Watershed Sciences Inc., Portland, Oregon, USA, 2003.

2065

- Burckholder, B. K., Grant, G. E., Haggerty, R., Khangaonkar, T., and Wampler, P. J.: Influence of hyporheic flow and geomorphology on temperature of a large, gravel bed river, Clackamas River, Oregon, USA, *Hydrol. Process.*, 22, 941–953, 2007.
- Bustillo, V., Moatar, F., Ducharne, A., Thiery, D., and Poirel, A.: A multimodel comparison for assessing water temperatures under changing climate conditions via the equilibrium temperature concept: case study of the Middle Loire River, France, *Hydrol. Process.*, 28, 1507–1524, 2014.
- Caissie, D.: The thermal regime of rivers: a review, *Freshwater Biol.*, 51, 1389–1406, 2006.
- Cardenas, B., Harvey, J. W., Packman, A. I., and Scott, D. T.: Ground-based thermography of fluvial systems at low and high discharge reveals potential complex thermal heterogeneity driven by flow variation and bio-roughness, *Hydrol. Process.*, 22, 980–986, 2008.
- Casado, A., Hannah, D. M., Peiry, J. L., and Campo, A. M.: Influence of dam-induced hydrological regulation on summer water temperature: Sauce Grande River, Argentina, *Ecohydrology*, 6, 523–535, 2013.
- Chander, G., Markham, B. L., and Helder, D. L.: Summary of current radiometric calibration coefficients for Landsat MSS, TM, ETM+ and EO-1 ALI sensors, *Remote Sens. Environ.*, 113, 893–903, 2009.
- Chapra, S. C.: *Surface Water-Quality Modeling*, Civil Engineering Series, McGraw-Hill International editions, Singapore, 1997.
- Cherkauer, K. A., Burges, S. J., Handcock, R. N., Kay, J. E., Kampf, S. K., and Gillepsie, A. R.: Assessing satellite based and aircraft based thermal infrared remote sensing for monitoring pacific northwest river temperature, *J. Am. Water Resour. As.*, 41, 1149–1159, 2005.
- Cristea, N. C. and Burges, S. J.: Use of thermal infrared imagery to complement monitoring and modeling of spatial stream temperatures, *J. Hydrol. Eng.*, 14, 1080–1090, 2009.
- Danielescu, S., MacQuarrie, K. T. B., and Faux, N. R.: The integration of thermal infrared imaging, discharge measurements and numerical simulation to quantify the relative contributions of freshwater inflows to small estuaries in Atlantic Canada, *Hydrol. Process.*, 23, 2847–2859, 2009.
- De Boer, T.: *Assessing the accuracy of water temperature determination and monitoring of inland surface waters using Landsat 7 ETM+ thermal infrared images*, MS thesis, Delft University, Delft, the Netherlands, 2014.

2066

- Desprez, N. and Martin, C.: Inventaire des points d'eau – piézométrie et bathymétrie des alluvions du lit majeur de la Loire entre Saint-Hilaire Saint-Mesmin et Saint-Laurent des Eaux, Rep. 76 SGN 461 BDP, BRGM, Orléans, France, 1976.
- Evans, E. C., McGregor, G. R., and Petts, G. E.: River energy budgets with special reference to river bed processes, *Hydrol. Process.*, 12, 575–595, 1998.
- Flipo, N., Monteil, C., Poulin, M., De Fouquet, C., and Krimissa, M.: Hybrid fitting of a hydrosystem model: long-term insight into the Beauce aquifer functioning (France), *Water Resour. Res.*, 48, W05509, doi:10.1029/2011WR011092, 2012.
- Gonzalez, R.: Étude de l'organisation et évaluation des échanges entre la Loire moyenne et l'aquifère des calcaires de Beauce, PhD thesis, Université d'Orléans, Orléans, France, 1991.
- Gutierrez, A. and Binet, S.: La Loire souterraine: circulations karstiques dans le val d'Orléans, *Géosciences*, 12, 42–53, 2010.
- Handcock, R. N., Gillepsie, A. R., Cherkauer, K. A., Kay, J. E., Burges, S. J., and Kampf, S. K.: Accuracy and uncertainty of thermal-infrared remote sensing of stream temperatures at multiple spatial scales, *Remote Sens. Environ.*, 100, 427–440, 2006.
- Handcock, R. N., Torgersen, C. E., Cherkauer, K. A., Gillepsie, A. R., Tockner, K., Faux, R. N., and Tan, J.: Thermal infrared sensing of water temperature in riverine landscapes, in: *Fluvial Remote Sensing for Science and Management*, 1st Edn., edited by: Carbonneau, P. E. and Piégay, H., John Wiley & Sons, Ltd., Chichester, UK, 2012.
- Hannah, D. M., Malcolm, I. A., Soulsby, C., and Youngson, A. F.: Heat exchanges and temperatures within a salmon spawning stream in the Cairngorms, Scotland: seasonal and sub-seasonal dynamics, *River Res. Appl.*, 20, 635–652, 2004.
- Hannah, D. M., Malcolm, I. A., Soulsby, C., and Youngson, A. F.: A comparison of forest and moorland stream microclimate, heat exchanges and thermal dynamics, *Hydrol. Process.*, 22, 919–940, 2008.
- Kay, J. E., Kampf, S. K., Handcock, R. N., Cherkauer, K. A., Gillepsie, A. R., and Burges, S. J.: Accuracy of lake and stream temperatures estimated from thermal infrared images, *J. Am. Water Resour. As.*, 41, 1161–1175, 2005.
- Lamaro, A. A., Marinelarena, A., Torrusio, S. E., and Sala, S. E.: Water surface temperature estimation from Landsat 7 ETM+ thermal infrared data using the generalized single-channel method: case study of Embalse del Rio Tercero (Cordoba, Argentina), *Adv. Space Res.*, 51, 492–500, 2013.

2067

- Latapie, A., Camenen, B., Rodrigues, S., Paquier, A., Bouchard, J. P., and Moatar, F.: Assessing channel response of a long river influenced by human disturbance, *Catena*, 121, 1–12, 2014.
- Loheide, S. P. and Gorelick, S. M.: Quantifying stream-aquifer interactions through the analysis of remotely sensed thermographic profiles and in-situ temperature histories, *Environ. Sci. Technol.*, 40, 3336–3341, 2006.
- Mallast, U., Gloaguen, R., Friesen, J., Rödiger, T., Geyer, S., Merz, R., and Siebert, C.: How to identify groundwater-caused thermal anomalies in lakes based on multi-temporal satellite data in semi-arid regions, *Hydrol. Earth Syst. Sci.*, 18, 2773–2787, doi:10.5194/hess-18-2773-2014, 2014.
- Mardhel, V., Frantar, P., Uhan, J., and Andjelov, M.: Index of development and persistence of the river networks (IDPR) as a component of regional groundwater vulnerability assessment in Slovenia, in: *Proceedings on the International Conference on Groundwater vulnerability assessment and mapping*, 15–18 June, Ustron, Poland, 2004.
- Moatar, F. and Gailhard, J.: Water temperature behaviour in the river Loire since 1976 and 1881, *Surf. Geosci.*, 338, 319–328, 2006.
- Monk, W. A., Wilbur, N. M., Curry, R. A., Gagnon, R., and Faux, R. N.: Linking landscape variables to cold water refugia in rivers, *J. Environ. Manage.*, 1, 170–176, 2013.
- Monteil, C.: Estimation de la contribution des principaux aquifères du bassin versant de la Loire au fonctionnement hydrologique du fleuve à l'étiage, PhD thesis, Mines Paris Tech, Paris, France, 2011.
- Putot, E. and Bichot, F.: CPER 2000–2006 Phase 4 – Modèle Infra-Toarcien Dogger: calage du modèle hydrodynamique en régime transitoire, Rep. BRGM/RP 55742-FR, BRGM, Orléans, France, 2007.
- Quintana-Segui, P., Moigne, P. L., Durand, Y., Martin, E., Habets, F., Baillon, M., Canellas, C., Franchisteguy, L., and Morel, S.: Analysis of near surface atmospheric variables: validation of the SAFRAN analysis over France, *J. Appl. Meteorol. Clim.*, 47, 92–107, 2008.
- Robinson, I. S., Wells, N. C., and Charnock, H.: The sea surface thermal boundary layer and its relevance to the measurements of sea surface temperature by airborne and spaceborne radiometers, *Int. J. Remote Sens.*, 5, 19–45, 1984.
- Salencon, M. J. and Thébaud, J. M.: Modélisation d'écosystème lacustre, Masson, Paris, France, 1997.

2068

- Smikrud, K. M., Prakash, A., and Nichols, J. V.: Decision-based fusion for improved fluvial landscape classification using digital aerial photographs and forward looking infrared images, *Photogramm. Eng. Rem. S.*, 74, 903–911, 2008.
- Sophocleous, M.: Interactions between groundwater and surface water: the state of science, *Hydrogeol. J.*, 10, 52–67, 2002.
- 5 Tonolla, D., Acuna, V., Uehlinger, U., Frank, T., and Tockner, K.: Thermal heterogeneity in river floodplains, *Ecosystems*, 13, 727–740, 2010.
- Torgersen, C. E., Price, D. M., Li, H. W., and McIntosh, B. A.: Multiscale thermal refugia and stream habitat associations of Chinook salmon in northeastern Oregon, *Ecol. Appl.*, 9, 301–319, 1999.
- 10 Torgersen, C. E., Faux, R. N., McIntosh, B. A., Poage, N. J., and Norton, D. J.: Airborne thermal remote sensing for water temperature assessment in rivers and streams, *Remote Sens. Environ.*, 76, 386–398, 2001.
- US Geological Survey: Landsat-A Global Land-Imaging Mission, US Geological Survey Fact sheet, Sioux Falls, Dakota, USA, p. 4, 2012, revised: 30 May 2013.
- 15 Wang, L. T., McKenna, T. E., and DeLiberty, T. L.: Locating ground-water discharge areas in Rehoboth and Indian River bays and Indian River, Delaware, using Landsat 7 imagery, Report of investigation no. 74, Delaware geological survey, Newark, State of Delaware, USA, 2008.
- 20 Ward, J. V.: *Aquatic Insect Ecology, Part I, Biology and Habitat*, Wiley & Son, New York, USA, 1992.
- Wawrzyniak, V.: *Etude multi-échelle de la température de surface des cours d'eau par imagerie infrarouge thermique: exemples dans le bassin du Rhône*, PhD thesis, Université Jean-Moulin, Lyon, France, 2012.
- 25 Wawrzyniak, V., Piégay, H., and Poiré, A.: Longitudinal and temporal thermal patterns of the French Rhône River using Landsat ETM+ thermal infrared (TIR) images, *Aquat. Sci.*, 74, 405–414, 2012.
- Wawrzyniak, V., Piégay, H., Allemand, P., Vaudor, L., and Grandjean, P.: Prediction of water temperature heterogeneity of braided rivers using very high resolution thermal infrared (TIR) images, *Int. J. Remote Sens.*, 34, 4812–4831, 2013.
- 30 Webb, B. W. and Zhang, Y.: Spatial and seasonal variability in the components of the river heat budget, *Hydrol. Process.*, 11, 79–101, 1997.

2069

- Webb, B. W. and Zhang, Y.: Water temperatures and heat budgets in Dorset chalk water courses, *Hydrol. Process.*, 13, 309–321, 1999.

2070

**Table 1.** Loire River temperature, air temperature and river flow at the date and hour when satellite images were taken.

Date	Daily river flow in Orléans (m <sup>3</sup> s <sup>-1</sup> )	Hourly mean water temperature in Dampierre (°C)	Hourly mean water temperature in Saint-Laurent des Eaux (°C)	Hourly air temperature in Orléans (°C)
<b>Winter</b>				
15 Nov 2001	182	5.2	5.75	5.65
22 Feb 2003	478	4.15	5.55	12.65
<b>Summer</b>				
29 May 2003	88.6	22.85	20.05	25.55
19 Jul 2010	112	23.4	23.1	28.25
20 Aug 2010	77.9	21.8	20.95	28.29
24 Aug 2000	83.3	24	22.55	30.45
29 Jul 2002	61.1	28.3	26	32.5

2071

**Table 2.** Details of the atmospheric heat fluxes calculations.

Solar radiations	RS estimated from the SAFRAN database	
Atmospheric radiations	$RA = \sigma \cdot (T_a + 273.15)^4 \cdot (A + 0.031 \cdot \sqrt{e_a}) \cdot (1 - R_L)$	$T_a$ (°C) is the air temperature estimated from the SAFRAN database from Météo France $\sigma = 4.9 \times 10^{-8} \text{ J m}^{-2} \text{ d}^{-1} \text{ K}^{-4}$ is the Stefan-Boltzman constant $A = 0.6R_L = 0.03$ are attenuation and reflection coefficients $e_a = 1.22 \times Q_a$ is the air vapour pressure $Q_a$ in $\text{g kg}^{-1}$ is the air specific humidity estimated from the SAFRAN database
Emitted radiations	$RE = \varepsilon \cdot \sigma \cdot (T_w + 273.15)^4$	$\varepsilon = 0.98$ water emissivity $T_w$ (°C) mean water temperature on the section estimated from the thermal longitudinal profiles
Conduction	$CV = \rho_a \cdot C_a \cdot e(V) \cdot (T_w - T_a)$	$\rho_a = 1.293 \cdot (\frac{273.15}{T})^3$ air density in $\text{kg m}^{-3}$ is function of air temperature $T$ (K) estimated from the SAFRAN database $C_a = 1002 \text{ J kg}^{-1} \text{ °C}^{-1}$ is the air specific heat $e(V) = 0.0025 \times (1 + V_2)$ is function of the wind 2 m above the ground $V_2$ ( $\text{m}^3 \text{ s}^{-1}$ ) $V_2 = V_{10} \cdot (\frac{2}{10})^{0.11}$ is used to estimate the wind 2 m above the ground as a function of the wind 10 m above the ground, itself estimated from the SAFRAN database
Condensation/ Evaporation	$CE = L(T_w) \cdot \rho_a \cdot e(V) \cdot (Q_w - Q_a)$	$L(T_w) = (2500.9 - 2.365 \cdot T_w) \cdot 10^3 \text{ J kg}^{-1}$ Is the latent evaporation heat $Q_w = \frac{4.596 \cdot e^{\frac{237.317}{T_w}}}{1.22}$ $Q_w$ in $\text{g kg}^{-1}$ is the specific humidity of the saturated air at the water temperature

2072

**Table 3.** Standard deviation of water temperature (°C) estimated on 200 m sections of the Loire River, with either under 20 water pixels in the section or over 20 water pixels.

Date	24 Aug 2000	15 Nov 2001	29 Jul 2002	22 Feb 2003	29 May 2003	19 Jul 2010	20 Aug 2010
$\sigma(n < 20)$	0.7	0.56	0.76	0.32	0.45	0.42	0.52
$\sigma(n > 20)$	0.5	0.44	0.73	0.26	0.41	0.41	0.42

2073

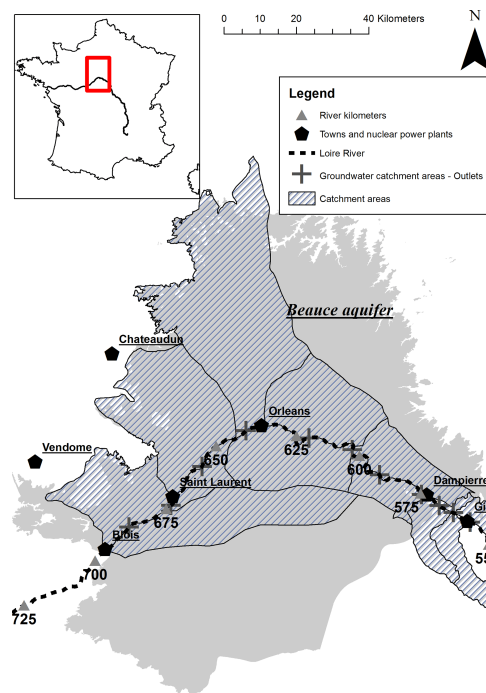


**Figure 1.** Map of the study area. The delineation of the Beauce aquifer comes from the BDLISA database from the Bureau de Recherches Géologiques et Minières (BRGM).

2074







